nederlands akoestisch genootschap
NAG

Journaal

nr. 202
november 2013

The application of efficient axisymmetric wave based models for the evaluation of the reflection coefficient of poro-elastic materials

Elke Deckers, Rene Boonen, Dirk Vandepitte, Wim Desmet
Department of Mechanical Engineering, Faculty of Engineering, KU Leuven, Celestijnenlaan 300B box 2420, 3001 Leuven (Heverlee), Belgium

Abstract

Performance metrics of poro-elastic materials such as sound absorption and the reflection coefficient are often obtained from impedance tube measurements. By measuring the acoustic pressure in two microphone locations, these frequency-dependent values can be obtained with simple expressions. However, these expressions are based on the assumption that the dynamic fields behave unidimensionally, which only holds in the case the sample is loosely fitting in the measurement tube and no air gaps are being present. As it is shown in various studies, the mounting conditions of the sample in the tube may have an important impact. Recently, a Wave Based Method has been developed to predict the dynamic behaviour of poro-elastic materials in a computationally efficient manner as compared to standard element based prediction techniques. This method can be straightforwardly applied to axisymmetric problems and allows evaluating the effect of mounting conditions. The potential of the proposed method is illustrated by comparing it to analytical expressions, finite element calculations and measurements.

1. Introduction

Poro-elastic media constitute a wide class of fibrous, granular cellular materials characterised by the fact that they consist of a solid frame and a fluid filling the voids. These materials are often applied in sound and vibration damping applications as energy can be dissipated effectively by structural, thermal and viscous means. A commonly applied mathematical model to describe the dynamic behaviour of such materials is the theory presented by Biot [1,2]. This theory applies a homogenised solid and a compressible fluid continuum description on the macroscopic level. This is justified when the characteristic dimensions of the material are small as compared to the wavelengths. Using a set of two frequency-dependent coupled partial differential equations, the constitutive Biot model predicts the existence of three different fluid-frame coupled wave types: a shear wave and two compressional waves.

Often simplified models are being applied. When it is assumed that the poro-elastic material has a rigid, motionless or a limp frame, only one wave type can propagate in the porous material. Its general acoustic behaviour can then be described using the Helmholtz equation and frequency dependent fluid properties. Within the limp model, the elasticity of the frame is neglected but the mass is accounted for. Different models can be found in literature and an overview is given in [2,3]. In this paper, the model of Johnson et al., Champoux and Allard is being considered.

End-users of poro-elastic materials are often interested in performance metrics such as acoustic impedance and acoustic absorption. Often, these data are obtained from impedance tube measurements. By measuring the acoustic pressure in two microphone locations, these

frequency-dependent values can be obtained using simple expressions. However, these expressions are based on the assumption that the dynamic fields behave one dimensionally. This assumption only holds in the case the sample is loosely fitting in the measurement tube and no air gaps are present. As has been shown in various studies, e.g. see [4], the mounting conditions can have an important impact. To account for these effects, analytical expressions are insufficient to accurately predict the dynamic behaviour in certain frequency ranges and numerical prediction techniques should be applied.

Nowadays, the Finite Element Method (FEM) is most commonly used to model the vibro-acoustic behaviour of those materials. Many formulations exist, of which the ($\mathbf{u}^s$,$\mathbf{u}^f$) [5] and the ($\mathbf{u}^s$,p)-formulation [6] are the most well-known. Although the FEM allows a great geometrical flexibility, its use is, however, restricted to the low frequency range due to the high number of unknowns per node and the fine meshes required to accurately capture the wave fields.

The family of Trefftz approaches follow a different scheme. *A priori* known information about the solution is embedded in the approximation expansion of the dynamic field variables. The Wave Based Method [7] belongs to this category of approaches. Recently it has been extended to also solve the Biot equations in a more efficient manner [8]. The Wave Based Method (WBM) partitions the problem domain into a small number of large, convex subdomains, contrarily to FEM. Within each subdomain, the dynamic field variables are described using a weighted sum of wave functions, which are exact solutions of the governing partial differential equations. The wave functions may, however, violate the imposed boundary and interface conditions. The errors on these are minimised using a weighted integral approach. The resulting matrices are small and the convergence rate of the method is high in comparison to FEM. Consequently, the method can be used up to higher frequencies. In the specific case of the Biot equations, the three wave types existing in poro-elastic materials are explicitly used. All dynamic field variables, such as displacements and stresses in both phases of the material, can be approximated using a superposition of three sets of globally defined wave functions [8]. For the specific case of impedance tube models, the efficiency of the WBM can be further increased. In [9] axisymmetric acoustic and poro-elastic wave functions have been derived. Only a slice of the tube needs to be modelled to obtain the dynamic solution, instead of a full 3-D model. Its high convergence rate as compared to axisymmetric FE models has been illustrated in [9].

This paper discusses the use of the axisymmetric WBM to evaluate the effect of mounting conditions of a poro-elastic sample in an impedance tube for absorption measurements. First the problem setting, including the governing equations is briefly discussed. The modelling procedure of the axisymmetric WBM for acoustic as well as poro-elastic problems is briefly discussed in the next chapter. The fourth chapter applies the methodology on a real Kundt tube setup and the results are compared to measurements. Also results obtained using equivalent fluid models are shown and the differences are explained.

2. Problem description

This section briefly describes the mathematical problem setting for a general axisymmetric acoustic-poro-elastic problem. The whole setting, including geometry, material properties, boundary and loading conditions are assumed to be independent of the circumferential coordinate, θ. It is as a consequence sufficient to study the dynamic in an axisymmetric section with (r,z)-coordinates. A time harmonic dependence $e^{j\omega t}$ is assumed with j the imaginary unit, ω the radial frequency and t the time. When a Kundt tube is considered, the total problem domain can be divided into one subdomain containing an acoustic and one

subdomain containing a poro-elastic media. This chapter briefly reviews the governing equations and the applied boundary and coupling conditions within this paper.

2.1 Acoustic problem description

The steady-state dynamic acoustic pressure is, in the absence of acoustic sources, given by the Helmholtz equation:

$$\nabla^2 p(\mathbf{r}) + k^2 p(\mathbf{r}) = 0, \tag{1}$$

where ∇^2 is the Laplace operator and $k=\omega/c$ is the acoustic wave number. Since the Helmholtz equation is a second-order differential equation, one boundary condition needs to be imposed at each point of the boundary in order to obtain a well-posed problem. In this paper only imposed normal velocity boundary conditions, and coupling conditions with a poro-elastic material are considered in this paper. The former is given by:

$$\frac{j}{\rho_0 \omega}\frac{\partial p(\mathbf{r})}{\partial \mathbf{n}} - \overline{v}_n(\mathbf{r}) = 0, \tag{2}$$

with ∂/∂n the normal derivative and $\overline{v}_n(\mathbf{r})$ the prescribed normal acoustic velocity. The coupling conditions with a poro-elastic domain will be explained in section 2.3.

2.2 Poro-elastic problem description

Poro-elastic materials consist of two constituents, i.e. the elastic frame and the fluid contained within the pores. The Biot theory [1] assumes that the pores are homogenously distributed in the material and describes the solid frame as an equivalent solid continuum phase and the fluid as an equivalent compressible fluid phase on a macroscopic level, being justified if the typical pore dimensions are very small as compared to the wavelength of sound. The acoustic energy is carried through the fluid in the pores as well as through the solid frame. According to the Biot theory the momentum equations may be written as

$$\nabla\cdot\sigma^s(\mathbf{r}) = -\omega^2\rho_1\mathbf{u}^s(\mathbf{r}) - (\omega^2\rho_a - j\omega b)(\mathbf{u}^s(\mathbf{r}) - \mathbf{u}^f(\mathbf{r})), \tag{3}$$

$$\nabla\cdot\sigma^f(\mathbf{r}) = -\omega^2\rho_2\mathbf{u}^f(\mathbf{r}) - (\omega^2\rho_a - j\omega b)(\mathbf{u}^f(\mathbf{r}) - \mathbf{u}^s(\mathbf{r})), \tag{4}$$

where the superscript *s*(*f*) indicates that variables are related to the solid (fluid) phase. In this paper the model of Johnson et al. and Champoux and Allard [2] is being applied to account for viscous and thermal dissipation. All material properties and field variables are detailed in [1,2,8]. The constitutive equations are:

$$\sigma^s(\mathbf{r}) = [(\lambda + Q^2/R)e^s(\mathbf{r}) + Qe^f(\mathbf{r})]\mathbf{I} + 2N\mathbf{e}^s(\mathbf{r}), \tag{5}$$

$$\sigma^f(\mathbf{r}) = [Qe^s(\mathbf{r}) + \mathrm{R}\, e^f(\mathbf{r})]\mathbf{I}, \tag{6}$$

The substitution of equations (3)-(4) into equations (5)-(6) leads to two coupled partial differential equations, describing the coupled dynamic behaviour between both phases.
As noted by Biot [1], it is known that porous materials can sustain three wave types simultaneously, two dilatational and one rotational, which interact and contribute significantly to the acoustic behaviour, depending on the considered frequency range, the boundary conditions considered and the excitation.
Three boundary conditions need to be imposed on each point of the boundary of the poro-elastic domain to have a uniquely defined problem. This paper studies two possible ways to

mount a sample in the Kundt tube: loosely fitting and fixed. In the former case sliding edge boundary conditions (mixed boundary conditions) are applied:

$$\begin{cases} u^s{}_n(\mathbf{r}) = 0 \\ u^f{}_n(\mathbf{r}) = 0 \\ \sigma^s{}_{ns}(\mathbf{r}) = 0 \end{cases}. \tag{7}$$

For fixed boundary conditions, the displacements of the solid phase and the normal displacements of the fluid phases are constrained on each point of the boundary:

$$\begin{cases} u^s{}_n(\mathbf{r}) = 0 \\ u^s{}_s(\mathbf{r}) = 0 \\ u^f{}_n(\mathbf{r}) = 0 \end{cases}, \tag{8}$$

2.3 Coupling conditions on the acoustic-poro-elastic interface

On the interface between the acoustic domain and the poro-elastic material 4 interface conditions need to be satisfied:

$$\begin{cases} \sigma^s{}_n(\mathbf{r}) = -(1-\phi)\,p(\mathbf{r}) \\ \sigma^s{}_{ns}(\mathbf{r}) = 0 \\ \sigma^f(\mathbf{r}) = -\phi\,p(\mathbf{r}) \\ \dfrac{j}{\rho_0\omega}\dfrac{\partial p(\mathbf{r})}{\partial \mathbf{n}} = j\omega(\phi u^f{}_n(\mathbf{r}) + (1-\phi)u^s{}_n(\mathbf{r})) \end{cases}, \tag{9}$$

where ϕ is the porosity. The first three conditions impose equilibrium between the stresses in the solid/ fluid phase and the acoustic domain and are imposed on the poro-elastic domain. The final condition represents the continuity of the normal volume velocity and is imposed on the acoustic domain.

3. The Wave Based Method for axisymmetric problems

The WBM is a deterministic numerical prediction technique based on the indirect Trefftz principle [7]. It aims at relaxing the frequency limitations encountered using element based prediction schemes for dynamic problems that can be described as a generalised Helmholtz problems. It applies exact solutions of the governing differential equations to approximate the field variables. The errors on boundary and interface residuals are minimised using a Galerkin weighted residual approach. Large domains can be used, as long as they are convex. In this paper, axisymmetric WB models are used to model a poro-elastic sample mounted in a Kundt tube setup. The theoretical derivation of the wave function set and its convergence characteristics can be found in [9]. This chapter briefly summarises the WBM modelling procedure for axisymmetric acoustic-poro-elastic problems, which consists of four steps.

3.1 Partitioning of the problem domain

A sufficient condition for the WBM to converge is that the considered problem domains are convex [7]. Non-convex problem domains have to be partitioned into a number of convex subdomains. For an impedance tube setup, which inherently has a simple geometry, no additional partitioning besides the physical domains is required.

3.2 Approximation of the field variables

The acoustic pressure $p^{(\alpha)}$ inside an acoustic domain $\Omega^{(\alpha)}$ is approximated using a weighted sum of wave functions:

$$p^{(\alpha)}(r,z) \approx \hat{p}^{(\alpha)}(r,z) = \sum_{w_a=1}^{n_{w_a}} u^{(\alpha)}{}_{w_a} \Phi^{(\alpha)}{}_{w_a}(r,z) = \mathbf{\Phi^{(\alpha)T}}(r,z)\mathbf{u^{(\alpha)}}. \tag{20}$$

The column vector $\mathbf{\Phi^{(\alpha)}}(r,z)$ collects the axisymmetric wave functions and the column vector $\mathbf{u^{(\alpha)}}$ contains the wave function contribution factors, the degrees of freedom. Each wave function is *a priori* defined, such that it fulfils the axisymmetric Helmholtz equation (1). It has been shown that the following set (consisting of an *s*- and a *t*-subset) is convergent:

$$\Phi_{w_a}(r,z) = \begin{cases} \Phi_{w_{a,s}}(r,z) = J_0(k_{rw_{a,s}} r)\cos(k_{zw_{a,s}} z) \\ \Phi_{w_{a,t}}(r,z) = J_0(k_{rw_{a,t}} r)e^{(-jk_{zw_{a,t}} z)} \end{cases}, \tag{31}$$

where J_0 is the Bessel function of zero order and first kind and the following wave number components are used:

$$\begin{cases} (k_{rw_{a,s}}, k_{zw_{a,s}}) = \left(\sqrt{k^2 - (k_{zw_{a,s}})^2}, \dfrac{w_{a,1}\pi}{L_{a,z}} \right) \\ (k_{rw_{a,t}}, k_{zw_{a,t}}) = \left(\lambda_{w_{a,2}}, \pm\sqrt{k^2 - (k_{rw_{a,t}})^2} \right) \end{cases}, \tag{12}$$

with $L_{a,r}$ and $L_{a,z}$ the dimensions of the smallest bounding box circumscribing the considered problem domain and the coefficients wa,1=0,1,2,… The indices $w_{a,2}$=0,1,2,… are associated with positive roots $\lambda_{w_{a,2}}$ of $J_1(L_{a,r}r)$. In order to apply the WBM in a numerical scheme, the wave function set is truncated according to the rule presented in [9].

To apply the WBM for axisymmetric poro-elastic problems, the Biot equations are decoupled into three Helmholtz equations applying the Helmholtz decomposition of a vector field [2,9]. One obtains the following three decoupled equations:

$$\begin{aligned} &\left(\nabla^2 \varphi_1^s(\mathbf{r}) + k_1{}^2 \varphi_1^s(\mathbf{r})\right)\left(\nabla^2 \varphi_2^s(\mathbf{r}) + k_2{}^2 \varphi_2^s(\mathbf{r})\right) = 0 \\ &\left(\nabla^2 \psi^s(\mathbf{r})\mathbf{e}_\theta + k_t{}^2 \psi^s(\mathbf{r})\mathbf{e}_\theta\right) = \mathbf{0} \end{aligned}, \tag{43}$$

Where $\varphi^s(r)=\varphi^s{}_1(\mathbf{r})+\varphi^s{}_2(\mathbf{r})$ is the scalar potential phase and $\psi^s(\mathbf{r})$ is the vector potential of the solid phase. Expressions for the three wave numbers are given in [2].

Each of the three potentials can be approximated using a weighted sum of wave functions, similarly to (12). Each wave function has to satisfy the associated equation in (13). For the scalar potentials, this leads to similar expressions as in (11)-(12). However, sine functions are included as well to obtain a faster convergence, leading to an s-, t- and u- subset:

$$\Phi_{w_{\varphi_\bullet}}(r,z) = \begin{cases} \Phi_{w_{\varphi_\bullet,s}}(r,z) = J_0(k_{rw_{\varphi_\bullet,s}} r)\cos(k_{zw_{\varphi_\bullet,s}} z) \\ \Phi_{w_{\varphi_\bullet,t}}(r,z) = J_0(k_{rw_{\varphi_\bullet,t}} r)\sin(k_{zw_{\varphi_\bullet,t}} z) \\ \Phi_{w_{\varphi_\bullet,u}}(r,z) = J_0(k_{rw_{\varphi_\bullet,u}} r)e^{(-jk_{zw_{\varphi_\bullet,u}} z)} \end{cases}, \tag{54}$$

where (● can be 1 or 2), the wave number components are defined as:

$$\begin{cases} (k_{rw_{\varphi_\bullet},s}, k_{zw_{\varphi_\bullet},s}) = (k_{rw_{\varphi_\bullet},t}, k_{zw_{\varphi_\bullet},t}) \\ \qquad\qquad = \left(\sqrt{k_\bullet{}^2 - (k_{zw_{\varphi_\bullet},s})^2}, \dfrac{w_{\varphi_\bullet,1}\pi}{L_{pe,z}} \right) \\ (k_{rw_{\varphi_\bullet},u}, k_{zw_{\varphi_\bullet},u}) = \left(\lambda_{w_{\varphi_\bullet},2}, \pm\sqrt{k_\bullet{}^2 - (k_{rw_{\varphi_\bullet},u})^2} \right) \end{cases} , \tag{15}$$

where all symbols are defined analogously to the acoustic case. The wave functions associated to the vector potentials contain Bessel functions of the first kind and order since the governing equation contains and additional *-1/r²*-term as compared to the scalar Helmholtz equation [9]:

$$\Phi_{w_\psi}(r,z) = \begin{cases} \Phi_{w_\psi,s}(r,z) = J_1(k_{rw_{\psi,s}} r)\cos(k_{zw_{\psi,s}} z) \\ \Phi_{w_\psi,t}(r,z) = J_1(k_{rw_{\psi,t}} r)\sin(k_{zw_{\psi,t}} z) \\ \Phi_{w_\psi,u}(r,z) = J_1(k_{rw_{\psi,u}} r) e^{(-jk_{zw_{\psi,u}} z)} \end{cases} , \tag{66}$$

using the following wave number components:

$$\begin{cases} (k_{rw_{\psi},s}, k_{zw_{\psi},s}) = (k_{rw_{\psi},t}, k_{zw_{\psi},t}) \\ \qquad\qquad = \left(\sqrt{k_t{}^2 - (k_{zw_{\psi},s})^2}, \dfrac{w_{\psi,1}\pi}{L_{pe,z}} \right) \\ (k_{rw_{\psi},u}, k_{zw_{\psi},u}) = \left(\lambda_{w_{\psi},2}, \pm\sqrt{k_t{}^2 - (k_{rw_{\psi},u})^2} \right) \end{cases} , \tag{17}$$

Applying analogous definitions. All wave functions that are strictly zero are excluded from the resulting wave function sets (e.g. the sine functions with wave number component zero). The truncation of the poro-elastic wave function sets is presented in [9].

3.3 Construction of the WB system matrices

Using the wave functions sets presented in the previous subsections for acoustic and poro-elastic problem domains, respectively, the governing equations are always satisfied, irrespective of the values of the unknown wave function contribution factors. These contributions factors are found by minimising the residuals on the boundary and interface conditions (2), (7)-(9). Each dynamic field variable, such as the acoustic velocity or poro-elastic displacements and stresses can be expressed in function of the wave function set(s) by applying differentiation operators [9]. The mutual interaction between the three wave field components in the poro-elastic domain is consequently entirely contained within the conditions specified along the boundary and interfaces. A Galerkin weighted residual approach is applied, similarly as in the FEM modelling procedure, leading to a fully populated and complex system of equations which can be solved for the unknown contribution factors. Details can again be found in [9].

3.4 Solution of the system of equations and post-processing

The final step in the WB modelling procedure is the solution of the system of equations, yielding the unknown contribution factors belonging to each wave function. The back substitution of these values into the field variable expansions yields an approximation of the

acoustic pressure field and the three poro-elastic potentials in each domain. Other quantities can be derived by applying differential operators on those wave function sets [9].

4. Numerical and experimental validation

In this section, the axisymmetric WBM is applied to predict the outcome of sound absorption measurements. It was shown in [9] that the WBM can accurately capture the effect of clamping conditions on the absorption coefficient of a poro-elastic material. In this chapter, different models for poro-elastic materials and measurements are compared and discussed.

A Fireflex foam, characterised by the Department of Physics of KU Leuven has been measured in a Kundt tube and simulated. Different models are used to this extent: the foam is modelled as a rigid frame material, a limp frame material, and as a poro-elastic material using the theory by Biot. For the first and second, which are equivalent fluid models, it is impossible to take into account clamping conditions, as the foam is modelled as fluid. Analytical expressions are used to obtain the sound absorption curves [2]. For the Biot models, two different mounting conditions are considered: sliding edge conditions (7) and fixed edge conditions (8). For the former, the sound absorption curve can be obtained analytically [2] as the field behaves one dimensionally; for the latter the WBM has been used.

The ambient pressure and temperature have been measured and the air properties are given in Table 1. The properties of the foam are given in Table 2 [10].

Table 1. Air material data.

Property	Value
Thermal conductivity	$2.6.10^{-2}$ W/(mK)
Specific heat capacity at constant pressure	$1.005.10^{3}$ J/(kgK)
Gas constant	$286.7 m^2/(s^2 K)$
Temperature	297.45K
Ratio of specific heats	1.4
Fluid kinematic viscosity	$15.5099.10^{-6}$ m^2/s
Fluid density	1.1949 kg/m^3

Table 2. Poro-elastic material data.

	Fireflex [9]
E_s	$(158+j17).10^{3}$ Pa
N	$(66+j3).10^{3}$ Pa
ρ_1	32 kg/m^3
ϕ	0.98
Λ	$1.8.10^{-4}$ m
Λ'	$3.6.10^{-4}$ m
σ	$8.9.10^{3}$ $kg/m^3 s$
α_∞	1.4

The setup is shown schematically in Figure 1. The axisymmetry axis is indicated by a dotted line. The diameter of the tube is 0.45 m, the length of the sample is 0.1 m and the microphones are separated by 0.05 m. The nearest microphone is at a distance of 0.089 m from the sample.

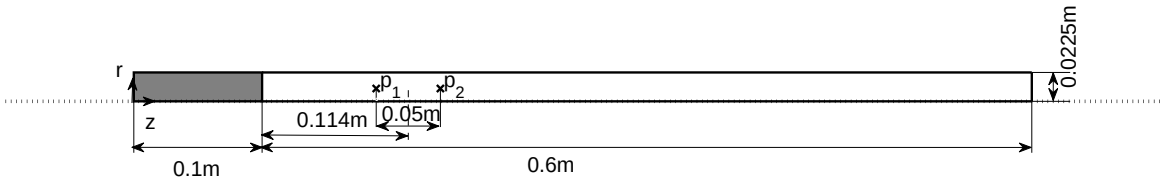

Figure 1: Problem description of the Kundt tube setup including the Fireflex sample.

The sample is glued to a rigid backing, applying fixed boundary conditions (8). The side wall of the measurement tube is assumed to be acoustically rigid: a normal acoustic velocity of 0 m/s has been applied, equation (2). The acoustic domain is excited with a normal velocity of 1 m/s, equation (2), at the right hand side of the acoustic domain, representing the loudspeaker. The length of the tube is 0.6m.

The damping in the acoustic domain is small, nevertheless is taken into account. The first order high frequency approximation of the acoustic wave number in a cylindrical pore is used within the acoustic domain, as explained in [9]. As such, viscous and thermal losses have been accounted for.

For the equivalent fluid models and the Biot model with sliding edge conditions, the absorption curves can be obtained using analytical expressions [2]. For the measurements and the Biot model with fixed edge mounting conditions, the pressure data at the microphone locations are post-processed to obtain the absorption coefficient. Hereto, following expressions are used, based again on the assumption that the dynamic fields behave 1-D. The absorption coefficient is defined as:

$$\alpha = 1 - |R|^2, \tag{77}$$

with R the reflection coefficient calculated using the obtained pressure $p(p_1)$ and $p(p_2)$ at the microphone locations:

$$R = \frac{e^{jkd_1} - e^{jkd_2}\, p(p_1)/p(p_2)}{e^{-jkd_2}\, p(p_1)/p(p_2) - e^{-jkd_1}}, \tag{18}$$

Figure 2 shows the absorption coefficient obtained by using the two equivalent fluid models. As also discussed in [11], at higher frequencies, both models agree very well. At lower frequencies, the limp model correctly takes into account the mass of the foam, giving a better prediction.

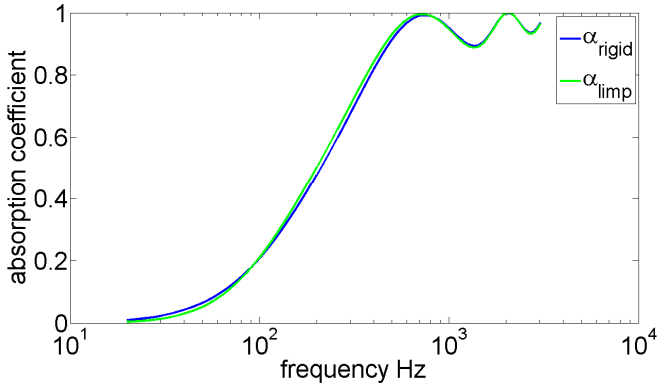

Figure 2: Absorption coefficient of the Fireflex sample, using two equivalent fluid models.

In Figure 3, two additional curves are added, representing the sound absorption curves obtained by the Biot model and applying sliding edge (7) and fixed edge (8) boundary conditions.

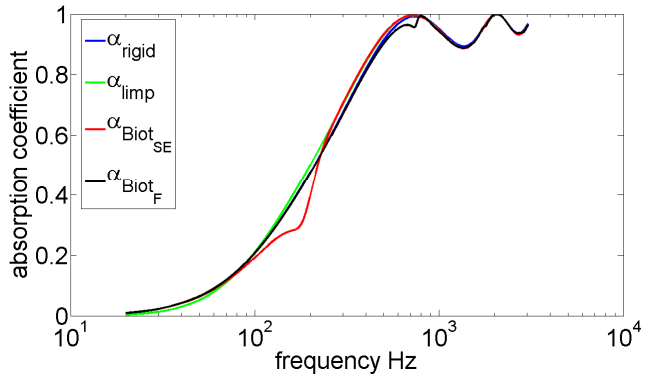

Figure 3: Absorption coefficient of the Fireflex sample, using two equivalent fluid models and the Biot theory applying sliding edge and fixed edge boundary conditions respectively.

As compared to the equivalent fluid models, the Biot models take into account the elasticity of the frame. Whereas the equivalent fluid models consider only one wave type (fluid compressional wave), the Biot model predicts the existence of three wave types: two compressional waves and one shear wave. The waves propagate simultaneously in both phases. However, at higher frequencies, the waves propagate predominantly in one phase and the terminology 'structure-borne' and 'airborne' wave are often used for the compressional waves. When the poro-elastic material is acoustically excited, at higher frequencies the frame is almost motionless due to its mass and it is mainly the 'airborne' wave that determines the behaviour of the foam. As can be seen, the red curve, which represents the absorption of the poro-elastic material when sliding edge conditions are applied, matches well with the equivalent fluid models at higher frequencies. Due to the mounting conditions, the shear wave is not excited. At the resonance frequency of the frame (slightly higher than 100Hz), however, the sound absorption is not well predicted by the equivalent fluid models. In the case the sample is clamped inside the Kundt tube, the sample behaves much stiffer and also the shear wave is excited. The dip due to the frame resonance shifts towards higher frequencies.

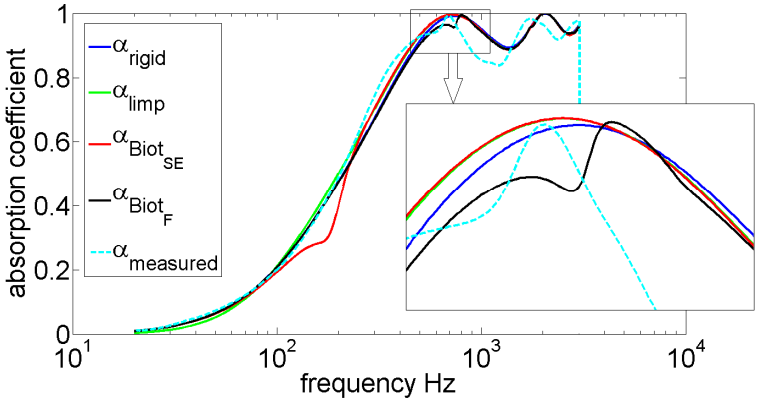

Figure 4: Absorption coefficient of the Fireflex sample, using two equivalent fluid models, the Biot theory applying sliding edge and fixed edge boundary conditions respectively and measurements.

To validate the simulations, a sample was cut and placed in the Kundt tube. The diameter of the sample was 0.1 mm larger than the diameter of the tube such that no air gaps were present. Although the curves are not on top of each other, it is clear that the Biot model with fixed boundary conditions accurately grasps the different phenomena. Differences are probably due to material properties (mean values are used in the simulation, a standard deviation of approximately 10% was obtained on the material properties [11]) and the effect of static compression of the sample. Sound absorption measurements are frequently used for poro-elastic material identification [12]. In this case, equivalent fluid models are applied, as

the curves are much smoother. To prevent the motion of the frame, the so-called 'voodoo-technique' is often applied: needles are inserted in the foam. As such, the characteristic lengths and the tortuosity can be estimated using an inverse procedure.

Conclusion

This paper presents the use of an efficient axisymmetric Wave Based Method to evaluate the effect of mounting conditions of a sample in a Kundt tube on the obtained sound absorption curves.

The WBM uses analytical solutions of the governing axisymmetric Helmholtz and decoupled Biot equations, respectively, to approximate the dynamic field variables. As such, *a priori* known information on the physics of the problem is embedded in the solution scheme, leading to a more efficient solution as compared to FE schemes.

The validation section compares sound absorption curves obtained by equivalent fluid models, Biot models applying different boundary conditions and measurements. The differences are explained. The WBM allows to simulate the physical phenomena that play a role when the sample is clamped in the tube as the prediction agrees well with the measurements.

ACKNOWLEDGMENTS

Elke Deckers is a postdoctoral fellow of the Fund for Scientifc Research Flanders (F.W.O). Furthermore, the Research Fund KU Leuven is also gratefully acknowledged for its support.

References

[1] M.A. Biot, 1956, "The theory of propagation of elastic waves in a fluid-saturated porous solid. I: Low frequency range. II: Higher frequency range", J. Acoust. Soc. Am. 28, 168–191.

[2] J.F. Allard, N. Atalla, 2009, "Propagation of Sound in Porous Media: Modeling Sound Absorbing Materials", John Wiley & Sons, West Sussex, United Kingdom, second edition.

[3] E. Deckers, S. Jonckheere, D. Vandepitte and W. Desmet, 2013, Modelling techniques for vibro-acoustic dynamics of poroelastic materials, submitted for publication in Archives of Computational Methods in Engineering.

[4] T.E. Vigran, L. Kelders, W. Lauriks, P. Leclaire, T.F. Johansen, 1997, "Prediction and measurements of the influence of boundary conditions in a standing wave tube", Acta Acustica United with Acustica 83, 419–423.

[5] Y.J. Kang, J.S. Bolton, 1999, "Finite element modeling of isotropic elastic porous materials coupled with acoustical finite elements", J. Acoust. Soc. Am. 98, 635–643.

[6] N. Atalla, R. Panneton, P. Debergue, 2001, "Enhanced weak integral formulation for the mixed (u,p) poroelastic equations", J. Acoust. Soc. Am. 109, 3065–3068.

[7] B. Pluymers, B. Van Hal, D. Vandepitte, W. Desmet, 2007, "Trefftz-based methods for time-harmonic acoustics", Arch. Comput. Methods Engrg. 14, 343–381.

[8] E. Deckers, N.-E. Hörlin, D. Vandepitte, W. Desmet, 2012, "A Wave Based Method for the efficient solution of the 2D poroelastic Biot equations", Comput. Methods Appl. Mech. Engrg. 201–204, 245–262.

[9] E. Deckers, D. Vandepitte, and W. Desmet, 2013, "A Wave Based Method for the axisymmetric dynamic analysis of acoustic and poroelastic problems". Comput. Methods Appl. Mech. Engrg. 257, 1–16.

[10] J. Descheemaeker, 2011, "Elastic characterization of porous materials by surface and guided acoustic wave propagation analysis". KU Leuven, Departement of physics, PhD. thesis, Leuven.

[11] R. Panneton, 2007, "Comments on the limp frame equivalent fluid model for porous media", Acoust. Soc. Am. 122, 217-222.

[12] Y. Atalla, R. Panneton, 2005, "Inverse acoustical characterization of open cell porous media using impedance tube measurements", Canadian Acoust. 33, 11–24.